Optically-Pumped Semicoductor Disk Lasers with Intracavity Second-Harmonic Generation

Frank Demaria and Alexander Kern

In this contribution, we present experimental results of our research on frequency-doubled semiconductor lasers emitting in the visible spectral range. These lasers include a laser-diode pumped semiconductor laser chip in an extended resonator configuration with a critically phase-matched lithium triborate crystal. The use of a single-plate Lyot filter within the cavity leads to single-peak emission with a bandwith of 1 nm at a 20 dB clip-level. The achieved second-harmonic power emission of 407 mW at a wavelength of 485 nm is still limited by the incident pump power.

1. Introduction

Second harmonic generation (SHG) drastically expands the spectral range that can be accessed by semiconductor lasers. For most visible wavelengths, the optical output powers and similarly the luminous fluxes exceed the values which can be achieved by semiconductor lasers directly, provided they exist at all. Hence, the utilization of this technique enables suitable light sources for projection displays. Multi-Watt optical output powers in the yellow-orange [1], green [2,3], and blue [4] spectral range have already been published by different research groups.

Although electrically-pumped surface emitting lasers with extended cavity may be considered as the more straightforward approach for intracavity frequency doubling [6], a few drawbacks arise with that. Unlike optically pumped structures, even the best luminous fluxes that have been demonstrated with intracavity frequency-doubling of laser diodes do not exhibit a potential that is required in projection displays using single emitters for each color. This is due to some fundamental requirements which can poorly be fulfilled that way. In vertical emitting lasers, the only way to establish excitation in a volume which is necessary to provide gain for several watts of optical power emission is to pump an area with diameters of some hundreds of micrometers. For such large areas, high conversion efficiencies become crucial because otherwise, the reduced heat spreading in the immediate vicinity of the active area leads to a fatal temperature increase. Current injection goes ahead with ohmic losses, also homogeneous or Gaussian distributed carrier injection over the required large areas is not possible. Although elaborated doping techniques like modulation doping are used, an optical absorption which is at least one order of magnitude higher is inevitably introduced. On the other hand, optical pumping allows homogeneous carrier generation in large areas without any ohmic losses and the absence of any intentional doping in optically pumped structures leads to low optical absorption

losses and much higher outcoupling efficiencies. For these reasons it is possible to achieve optical output powers of more than 13 W, where the emitted power significantly exceeds the dissipated power in the structure [11].

2. Experimental Setup and Results

2.1 Experimental setup for intracavity second-harmonic generation

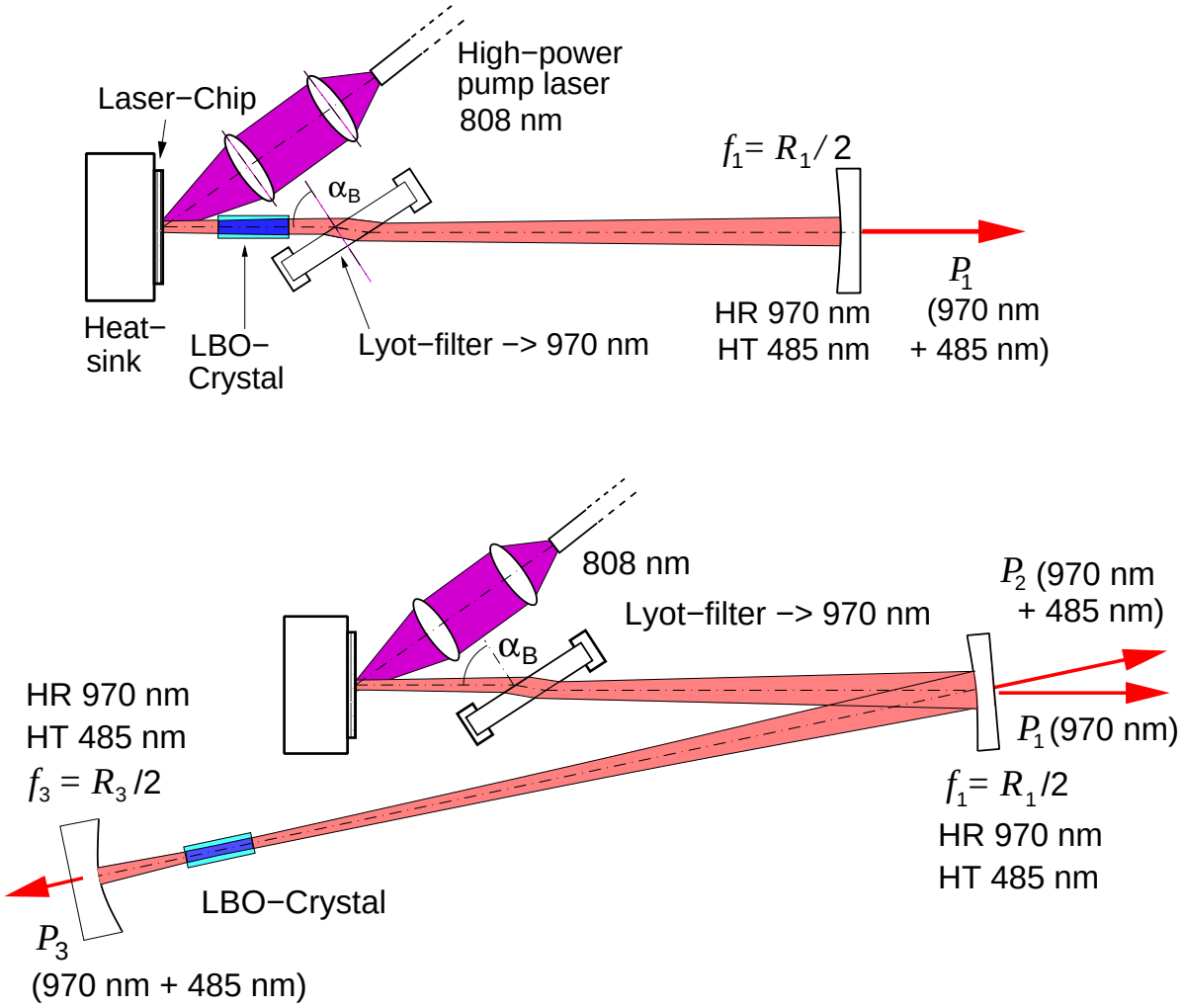

Fig. 1: Setup for intracavity second-harmonic generation with a hemispherical resonator (top) and a folded resonator (bottom).

Figure 1 is a schematic representation of the experimental setups. A simple hemispherical and a single-folded resonator configuration are used. The semiconductor laser chip is designed and fabricated for a pumping wavelength of 808 nm and an emission wavelength of 970 nm. It includes six strain compensated $In_{0.15}Ga_{0.85}As$ quantum wells and a double-band Bragg mirror [12]. The chip is mounted on a copper heat sink whose temperature

is stabilized at a value of 0 °C by a Peltier cooler. Optical pumping is realized by a fiber-coupled diode laser. The collimated output from a fiber with 200 µm core-diameter is focused by a 6 mm-diameter plano-convex lens with 12 mm focal length what results in a pump-spot diameter of approximately 110 µm. The inclination angle is 25 ° with respect to the surface normal.

Second harmonic generation is achieved by a 8 mm-long, $3 \times 3\,\mathrm{mm}^2$ cross-section lithium triborate crystal (LiB_3O_5, LBO) in a critically phase-matched configuration. The walk-off angle is 0.6 ° and the spectral acceptance 1 nm · cm. Spectral stability and small-banded single-peak emission is provided by a 2 mm-thick single-plate Lyot filter. The functionality of birefringent filters and their application in intracavity second-harmonic generation setups is extensively described in literature [7–10]. Here the most simple form consists of a plane-parallel plate made out of positive uniaxial crystal quartz with its optical axis parallel to the surface. The surface is oriented under the Brewster angle of approximately 57 °, hence TE-polarized radiation will partially be reflected. Accordingly, stimulated emission with that polarization is suppressed, whereas simultaneously the gain contribution to TM-polarization is strengthened. That way, a stable polarization is established, which is essential for efficient and stable critically phase-matched frequency doubling. Inside the quartz crystal, the radiation splits of into an ordinary and an extraordinary beam. The refractive index for the extraordinary beam is determined by the angle between the optical axis and the direction of polarization, which can be tuned by axial rotation of the filter. Thus, the phase shift between the ordinary and extraordinary beam is adjustable and simultaneously the resonance wavelength. In other words, the quartz plate acts as a tunable frequency filter.

2.2 Spectral behavior

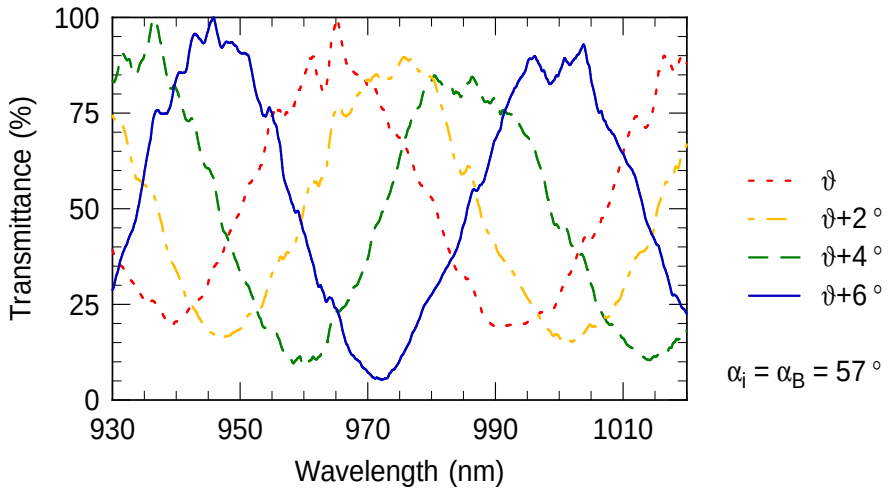

Fig. 2: Transmission spectra of a 2 mm-thick Lyot filter for an incident angle α_i of 57 ° (Brewster angle α_B). For the different spectra, the filter has been turned along its axial direction with a step size of 2 ° in the angle θ.

Figure 2 shows the measured transmission spectra of the 2 mm-thick Lyot filter. In this

measurement, it is located between two polarizers under the Brewster angle of 57° and transmitted by light from a thermal light source. Turning the filter along its axial direction results in a spectral shift of approximately 5.8 nm per angle-degree. The filter reveals a free spectral range of 52 nm between the transmission maxima. This is sufficient to assure single peak emission under all circumstances. This is not the case for a 4 mm-thick Lyot filter, as for certain pump intensities and angular orientations two discrete peaks with a distance of 25 nm can be observed.

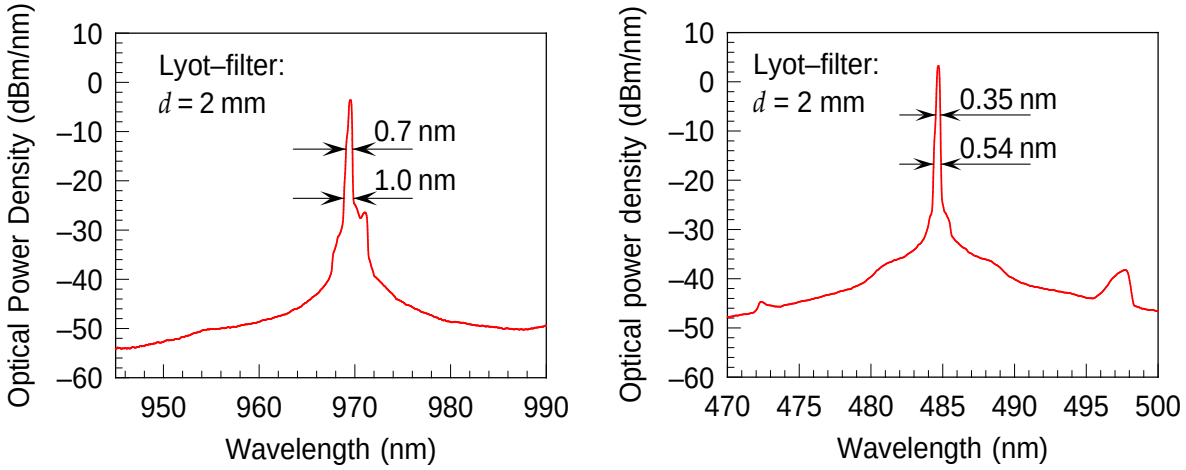

Fig. 3: Emission spectra from a laser configuration with a 2 mm-thick intra-cavity Lyot filter according to the top representation of Fig. 1. The left spectrum of fundamental emission reveals a width of 0.70 nm and 1.0 nm at a 10 dB and 20 dB-clip level. For the second harmonic spectrum on the left, the spectral widths are halved, together with the wavelength, so the relative width remains nearly unchanged.

In Fig. 3, the emission spectra from a linear resonator setup according to the top representation of Fig. 1 are shown. The spectrum of fundamental emission reveals a width of 0.70 nm at a 10 dB clip level and 1.0 nm at a 20 dB clip level. In the spectrum of the second harmonic, the relative width remains unchanged.

2.3 Output characteristics with a simple hemispherical resonator

In the single hemispherical resonator, an external mirror with 0.08 % transmittivity and a focal length of 50 mm is utilized. The resonator length is 92 mm. The output characteristics for the second harmonic and the fundamental optical output power is shown in Fig. 4. The spectral contribution to the output power is observed by the application of band-edge filters. The fundamental output power is also measured after removal of the LBO crystal. At an absorbed optical pump power of 7.5 W, the measurement was stopped to avoid the risk of a damage of the laser chip and to preserve it for further measurements. At this value, a second-harmonic optical output power of 260 mW is emitted, which corresponds to a conversion efficiency of 3.5 %. For each measurement point the LBO-crystal had to be re-adjusted. For discrete measurement points also the diffraction number M^2 of the second harmonic and also the fundamental emission is measured. Generally, the beam quality of the second harmonic exceeds the fundamental emission. This is because the

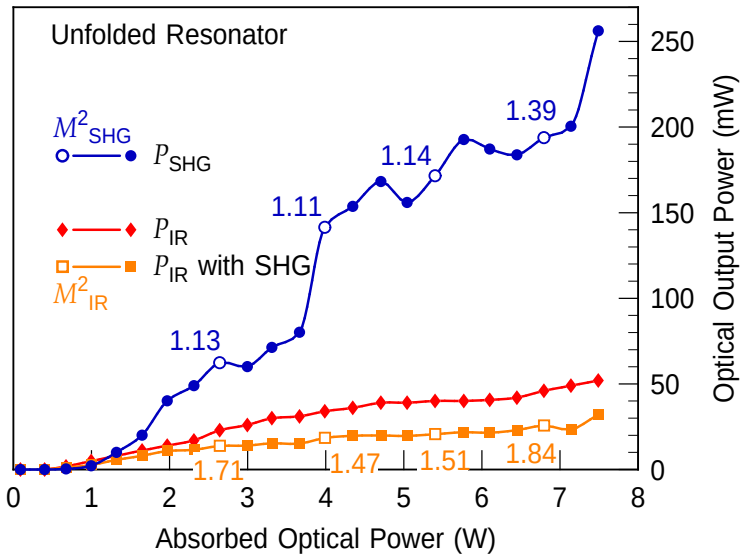

Fig. 4: Second harmonic optical output power and fundamental optical output power with and without SHG crystal. The 92 mm-long resonator with a single external mirror of 50 mm focal length and a transmittivity of 0.08 % includes a 2 mm-thick Lyot filter and a 8 mm-long LBO crystal. For individual measurement points the diffraction numbers M^2 which have also been determined are plotted.

fundamental TEM_{00}-mode and low order modes contribute more to the second harmonic generation due to their higher radiance.

2.4 Output characteristics with a folded resonator

All setups with a single folded resonator include a folding mirror with a focal length of $f_1 = 50$ mm and a transmittivity of 0.08 % at 970 nm. The chip-sided leg has a length of $L_1 \approx 91$ mm. The different end-mirrors with focal lengths of 15 mm and 50 mm have approximately a similar transmission characteristics as the folding mirror. Optical power emission is given by the sum of the different output powers P_1, P_2 and P_3, which refer to emission directions labeled in Fig. 1. In a more application-oriented setup, an end mirror with a high reflectivity for the second harmonic is recommended to assure that the second harmonic emission is predominantly coupled out of the folding mirror. In this case, the overall optical emission is approximately given by P_2. For each measurement point, the orientation of the LBO-crystal was adjusted.

The upper diagram of Fig. 5 refers to a 15 mm focal-length end mirror. A second harmonic output power of 220 mW and a conversion efficiency of 2.6 % is achieved at a maximum pump power of 8.3 W. The lower diagram of Fig. 5 refers to a 50 mm focal-length end mirror. There, at 6.8 W of absorbed optical power, a second harmonic power of 240 mW and a conversion efficiency of 3.5 % is achieved. At high pump powers, the slope of the second harmonic is increasing significantly. Comparison of the measured beam-quality shows that for the given pump-spot size, much better values are achieved for the resonator

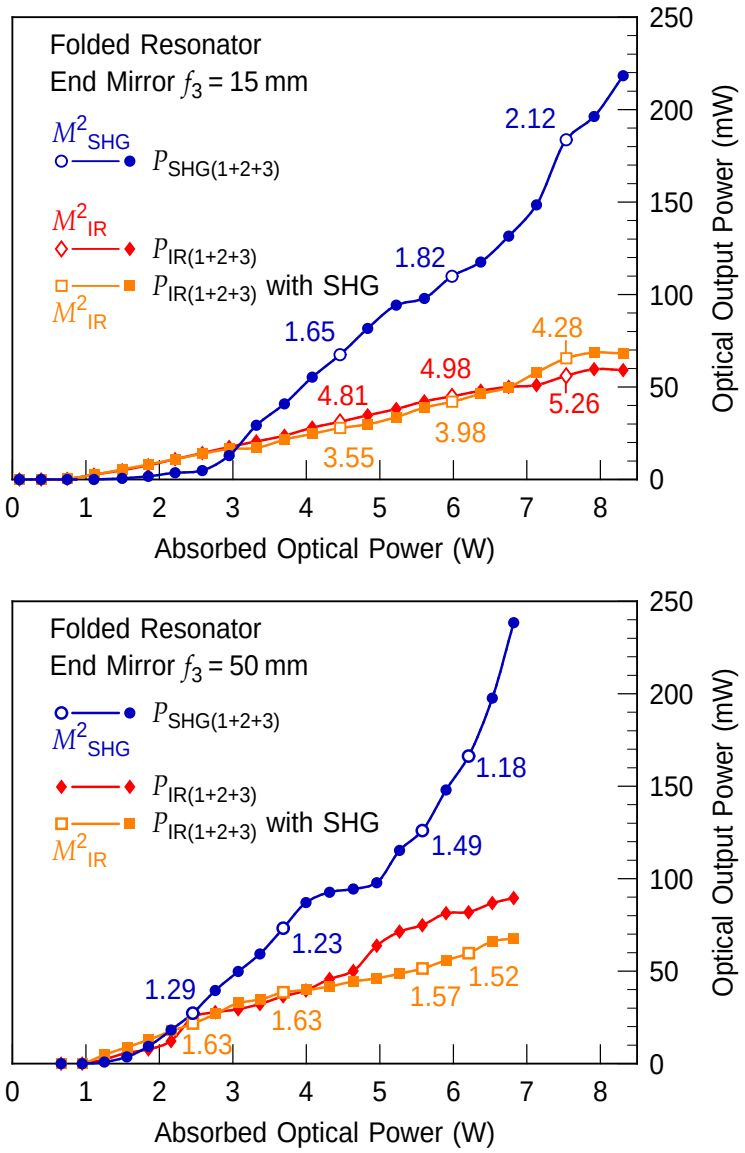

Fig. 5: Output characteristics of the second harmonic and the fundamental emission which is detected with and without the crystal. The upper diagram is based on a end-mirror with 15 mm focal length, in the lower diagram the end mirrors focal length is 50 mm.

geometry with the longer focal length. This is consistend with theoretical predictions [13].

With the described configuration, containing an end-mirror with 50 mm focal-length, an even better performance has been achieved in an independent measurement which is shown in Fig. 6. A maximum SHG output power of 407 mW is achieved, which was measured by the emission from the folded leg $P_2 + P_3$ at a pump power of 8.3 W. This results in a conversion efficiency of 4.9 %.

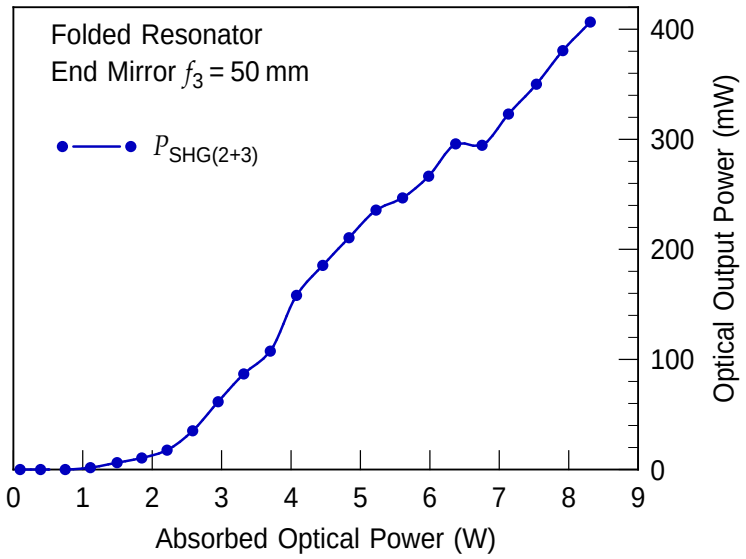

Fig. 6: Second harmonic output characteristics from a single folded resonator configuration. The emitted second harmonic output power $P_2 + P_3$ is 407 mW at an absorbed pump power of 8.3 W what results in a conversion efficiency of 4.9 %.

3. Conclusion and Outlook

We have demonstrated the capability to generate second harmonic output powers of several hundreds of milliwatts from semiconductor disk lasers which have been fabricated by our group. The optical output power was only limited by the applied pumping power. In the spectrum of the second harmonic, the relative spectral width of the fundamental emission peak remains nearly unchanged within a 20 dB level which indicates, that the SHG conversion efficiency is barely limited by the spectral width. Although on a laboratory scale, the setup size appears quite large, a reduction to much shorter dimensions is practicable. This can be done by applying a free-space pump scheme and a short cavity configuration with a nevertheless large mode volume within the gain medium [5]. Thus the described approach is particularly suitable for pocket-size projector displays and so called "pico projector displays".

References

[1] S. Hilbich, W. Seelert, V. Ostroumov, C. Kannengiesser, R. von Elm, J. Mueller, E. Weiss, H. Zhou, and J. Chilla, "New wavelengths in the yellow orange range between 545 nm to 580 nm generated by an intracavity frequency doubled optically pumped semiconductor laser," *Proc. SPIE*, vol. 6451, no. 64510C, 2007.

[2] S. Cho, G.B. Kim, J.-Y. Kim, K.-S. Kim, S.-M. Lee, J. Yoo, T. Kim, and Y. Park, "Compact and efficient green VECSEL based on novel optical end-pumping scheme," *IEEE Photon. Technol. Lett.*, vol. 19, no. 17, pp. 1325–1327, 2007.

[3] L. E. Hunziker, Q. Z. Shu, D. Bauer, C. Ilhi, G. J. Mahnke, M. Rebut, J. R. Chilla, A. L. Caphara, H. Zhu, E. S. Weiss, and M. K. Reed, "Power-scaling of optically-pumped semiconductor lasers," *Proc. SPIE*, vol. 6451, no. 64510A, pp. 1–6, 2007.

[4] G. Bum Kim, J.-Y. Kim, J. Lee, J. Yoo, K.-S. Kim, S.-M. Lee, S. Cho, S.-J. Lim, T. Kim, and Y. Park, "End-pumped green and blue vertical external cavity surface emitting laser devices," *Appl. Phys. Lett.*, vol. 89, no. 18, 181106, 2006.

[5] M. Schulze and A. Masters, "Optically pumped semiconductor lasers expand the scope of potential applications," *Laser Focus World*, vol. 42, no. 21, pp. 77–80, 2006.

[6] E.U. Rafailov, W. Sibbett, A. Mooradian, J.G. McInerney, H. Karlsson, S. Wang, and F. Laurell, "Efficient frequency doubling of a vertical-extended-cavity surface-emitting laser diode by use of a periodically poled KTP crystal," *Opt. Lett.*, vol. 28, no. 21, pp. 2091–2093, 2003.

[7] J.W. Evans, "The birefringent filter," *J. Opt. Soc. Am.*, vol. 39, no. 3, p. 229, 1949.

[8] M. Jacquemet, M. Domenech, G. Lucas-Leclin, P. Georges, J. Dion, M. Strassner, I. Sagnes, and A. Garnache, "Single-frequency cw vertical external cavity surface emitting semiconductor laser at 1003 nm and 501 nm by intracavity frequency doubling," *Appl. Phys. B*, vol. 86, pp. 503–510, 2007.

[9] R. Hartke, E. Heumann, G. Huber, M. Kühnelt, and U. Steegmüller, "Efficient green generation by intracavity frequency doubling of an optically pumped semiconductor disk laser," *Appl. Phys. B*, vol. 87, pp. 95–99, 2007.

[10] J. Lee, S.-M. Lee, T. Kim, and Y. Park, "7 W high-efficiency continuous-wave green light generation by intracavity frequency doubling of an end-pumped vertical external-cavity surface emitting semiconductor laser," *Appl. Phys. Lett.*, vol. 89, no. 241107, 2006.

[11] F. Demaria and M. Riedl, "High-radiance optically pumped semiconductor disk lasers," *Annual Report 2006, Institute of Optoelectronics, Ulm University*, pp. 3–9.

[12] E. Gerster, I. Ecker, S. Lorch, C. Hahn, S. Menzel, and P. Unger, "Orange-emitting frequency-doubled GaAsSb/GaAs semiconductor disk laser," *J. Appl. Phys.*, vol. 94, no. 12, pp. 7397–7401, 2003.

[13] F. Demaria, *Schicht- und Resonatordesign von Halbleiterscheibenlasern*. Ph.D. Thesis, Ulm University, 2008.